

# LOW ENERGY BEAM TRANSPORT DEVELOPMENT FOR THE BILBAO ACCELERATOR\*

I. Bustinduy, I. Rodriguez, Z. Izaola, J.L. Munoz, D. de Cos, J. Feuchtwanger, ESS-Bilbao, Spain  
V. Etxebarria, J. Portilla, F.J. Bermejo, UPV/EHU, Spain

## Abstract

In this work we present a future upgrade of the ESS-Bilbao multi-source Low Energy Transport System (LEBT). It consists of a set of solenoids and steering dipoles used to match the characteristics of both ion source beams i.e., the Electron Cyclotron Resonance (ECR)  $H^+/D^+$  source and the  $H^-$  Penning source, to the input specifications of the RFQ. Different configurations of the geometry and magnetic fields are studied in order to minimize the emittance growth along the LEBT, while providing the beam specifications required by the RFQ.

## INTRODUCTION

The ESS-Bilbao accelerator facility aims to transport and accelerate both  $H^+$  and  $H^-$  beams. The  $H^+$  beam, produced by means of an ECR ion source, is expected to generate a current of 75 mA, with a pulse length of up to 2 ms and a repetition rate of 50 Hz (max.). On the other hand the  $H^-$  beam produced by a Penning source will generate a current of 65 mA, a pulse length of 1.5 ms and a repetition rate of 50 Hz having a strong non-axisymmetric transverse profile. Being the task of the LEBT to match the beam characteristics with the specifications needed for the the RFQ, it becomes thus a crucial component of study and design within the accelerator.

Our first design of the LEBT was based on a revolver-type mechanism designed to transport both  $H^+$  and  $H^-$  beams [1]. The main drawback of this layout is that Ion Sources may not be plugged-in simultaneously and thus a considerable amount of time is wasted each time the Ion sources are switched and the accelerator has to be put back to operation. In order to reduce this time a new layout is presented here.

This work summarizes the latest advances on the possible future upgrade towards an Y-shaped LEBT design — similar to the one proposed in the SNS upgrade plans [2], which would allow for a rapid switching between the two ion sources. In this new layout two ion sources are connected by means of a sector magnet, where the rest of the components are planned to be recycled from the current design [1]. Several aspects of the future upgradability design status will be covered, including the magnetic structure and beam dynamics simulations.

\*Work supported by ESS-Bilbao

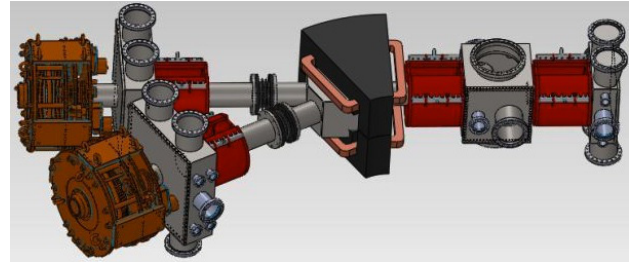


Figure 1: Low energy Beam Transport layout.

## AXISYMMETRIC SECTOR MAGNET

One of the key aspects for the upgradeability of the current design, is the reutilization of the components that comprise the former LEBT. There is however one component that has to be designed from scratch, i.e. the sector magnet.

In principle it is possible to preserve the axisymmetry of a beam after passing through a bending magnet, provided that the magnetic field is not purely dipolar (combined function magnet). For a sector magnet with a field gradient component the condition imposes the relation

$$g = -B_y/2\rho, \quad (1)$$

where  $\rho$  is the bending radius,  $B_y$  is the dipole field and  $g$  is the field gradient ( $\partial B_y/\partial x$ ). In the more general case of a sector magnet with a quadrupole component numerical solution of equations in ref. [3] should be obtained.

The minimum angle between the two incoming beams comes determined by the minimum separation gap that must exist between the high voltage platforms to prevent from high voltage breakdowns. This angle  $\phi$  can be inferred by the formula:

$$-l \times \cos(\phi/2) - d \times \sin(\phi/2) = a/2, \quad (2)$$

where  $d$  is the distance between the platform and the dipole,  $l$  is the distance from each ion source to the edge of its correspondent platform and  $a$  is the distance between the two platforms.  $a$  is determined by the dielectric breakdown of dry air ( $|V_{H^+} - V_{H^-}|/3.10^6$ ), which in our case sets a minimum threshold of 67 mm. For  $l = 500 \text{ mm}$  and  $d = 532.8 \text{ mm}$ , we obtain an estimated angle of  $30^\circ$ .

## Magnetic Model Setup

The dipole is defined as an H-type magnet, which improves the field quality and presents a low stray field. A

Beam Dynamics and EM Fields

Dynamics 01: Beam Optics (lattices, correction, transport)

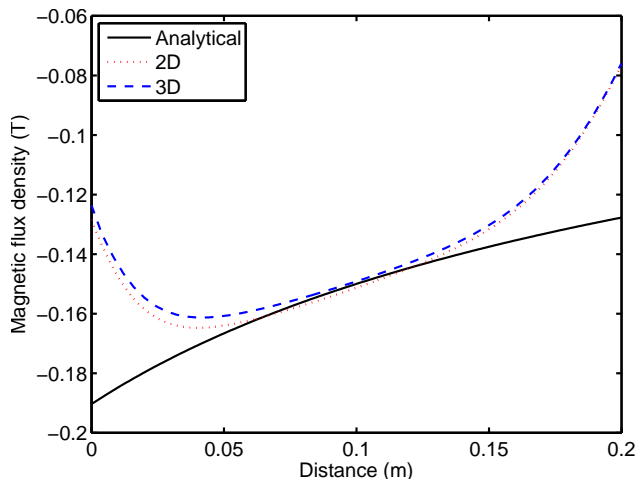


Figure 2: Radial magnetic field (T) at the aperture cross section, for the different calculations.

crucial parameter when designing a magnet is its minimum aperture. In order to fit a 100 mm diameter pipe, the aperture of the magnet has been estimated to be 104 mm. To avoid remnant magnetization problems, the minimum chosen dipolar field is 0.15 T. The magnetic rigidity of 75 keV  $H^-$  ions is 0.0396 T.m, which corresponds to a bending radius of 263.8 mm. Using the previously estimated bending angle of  $30^\circ$ , the required integrated field for the ideal particle is 20.7 mT/m, whereas the quadrupole component gradient for  $n = 1/2$  field index is 0.2843 T/m. A current of 6200 Ampere-turn is analytically estimated for this design. The average current density in the coil is fixed at  $5.2 \text{ A/mm}^2$ , this value simplifies the cooling by using flowing water through a hollow conductor. The dimensions of the iron have been calculated using the magnetic fluxes equality in each iron zone, bearing in mind the higher iron volume for a higher iron radius. Thus, the iron works at the same level of saturation, avoiding wasted material or excessive saturation of certain areas. The width of the poles is set at 200 mm. The theoretical field at the magnet aperture can be drawn using  $\beta_y = \beta_0(1 + x/\rho)^{-n}$  and is shown in Fig. 2. It consists of a steady dipole field of 0.15 T and a 0.2843 T/m quadrupole field gradient plus other high order multipoles. In a first approach the magnet can be described using a 2D finite elements model (FEM) due to its axisymmetric property around the axe. This way the aperture fields and the coil dimensions can be accurately described before tackling the problem with more sophisticated 3D simulations.

### 3D FEM simulations

COMSOL [4] uses the vector potential method to solve the 3D magnetostatic problem, and therefore there is no need to define the coils for the symmetric regions of the model. However, COMSOL needs to mesh the coils in the same way as the rest of the solids in the model, implying that the air space between the coils and the iron (which

### Beam Dynamics and EM Fields

#### Dynamics 01: Beam Optics (lattices, correction, transport)

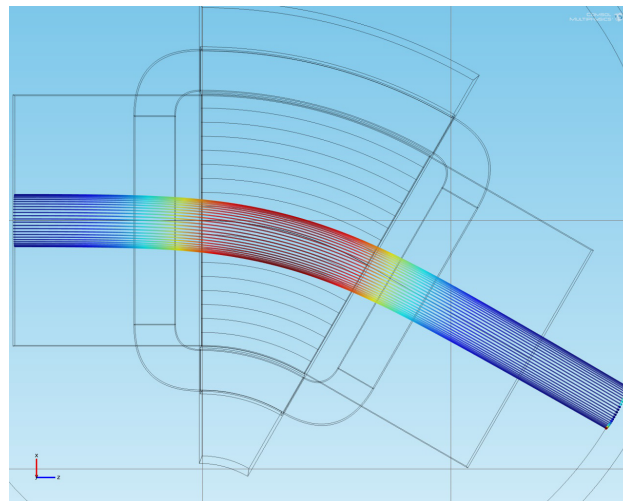


Figure 3: Trajectory of a set of particles in the reduced field magnet ( $\sim 57\%$ ).

is very narrow) requires some very specific meshing conditions to avoid possible artifacts in the solution. Fig. 2 shows the radial field at the aperture of the magnet calculated by COMSOL (2D and 3D), we have also included for comparison the lowest order analytical solution. Although the central field of the magnet is the desired one (0.15 T), the path shown in the Fig. 3 is affected by the dipole 3D coil-end effects. The fringing fields provide an additional deflection, increasing the integrated strength of the magnet and the magnetic length (the particles are deflected at the entrance and thus perform a wider angle turn). This 3D effect cannot be avoided unless one makes use of magnetic field clamps, and it should be commonly compensated by adjusting the value of the integrated field and displacing the ideal particle at the magnet entrance by the proper calculated distance [3]. The reduction of the magnetic field in the aperture by  $\sim 57\%$  in the presented model forces the ideal particle to enter and exit the magnet symmetrically, following the expected rectilinear beam paths before and after the magnet. Obviously, the described curve poses a radius bigger than the initially designed one. This means that the magnet presents the exactly required integrated force (20.7 mT.m) but with a longer magnetic length. A future update of the design will solve all these problems allowing a good focalization and deflection of the particles at the same time.

## BEAM DYNAMICS SIMULATIONS

To test the capability of the proposed Y-shaped LEBT lattice to match the transverse characteristics of the beam given in terms of the Courant-Snyder parameters as  $[T\alpha x, T\beta x, T\alpha y, T\beta y]$  to the RFQ input specification, two sets of simulations have been carried out. For both calculations, as usual for these cases, the transmission of the beam has been maximized and its emittance growth minimized. The  $H^+$  is a 75 mA/75 keV highly axisymmetric

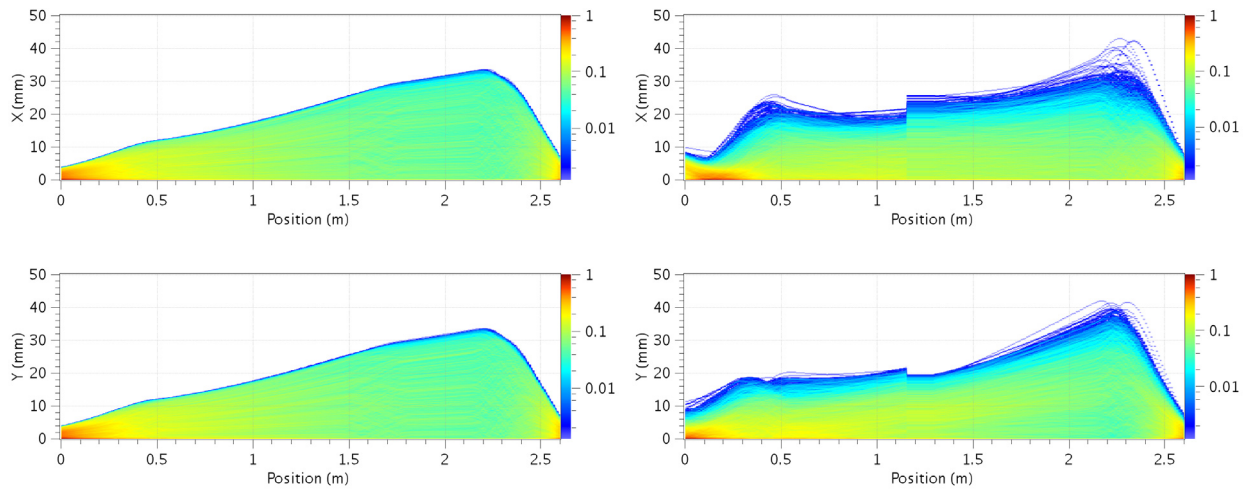


Figure 4: Transverse projection of the particles along the LEBT. Left frames:  $H^+$ . Right frames:  $H^-$ . Upper frames: Horizontal projections. Bottom frames: Vertical projections.

beam transported along the straight path. This beam is defined by [ $T\alpha_{xi} = -4.059$ ,  $T\alpha_{yi} = 4.094$ ,  $T\beta_{xi} = 1.283$  m/rad,  $T\beta_{yi} = 1.301$  m/rad], presenting an input normalized emittance of  $\sim 0.03$   $\pi$ -mm-mrad in both planes.

The  $H^-$  beam used for these simulations and transported along the bending magnet, is a 62 mA/70 keV scaled version of the measured one —within the ISIS-FETS project, using a pepperpot device [5]. This beam is defined by the following parameters:  $T\alpha_{xi} = 1.453$ ,  $T\alpha_{yi} = 0.080$ ,  $T\beta_{xi} = 0.296$  m/rad,  $T\beta_{yi} = 0.124$  m/rad, presenting a normalized emittance of  $\sim 0.6$   $\pi$ -mm-mrad in both planes.

TRACEWIN [6] was used to study the robustness of this lattice: The 3 solenoids can be tuned to achieve a perfect matching of the beam to the chopper entrance. Solenoid fields are in the range of 0.1 - 0.4 T. Two different 3D magnetic field maps, single and dipole-solenoid assemblies, were loaded in TRACEWIN to represent each family of solenoids; one for each specific branch and the other two for the shared section. Fig. 4 shows the trajectories of both 75 mA  $H^+$  and 62 mA  $H^-$  beams, simulated using a 90% charge neutralization transported through the LEBT and matched into the RFQ. The total length of the beam path is 2638 mm for both pipes  $H^+$  and  $H^-$ . Along each beam path, the rms beam diameter does not exceed  $\sim 11\%$  of the 130 mm aperture of the common section of the LEBT, and does not exceed the  $\sim 40\%$  (in the case of  $H^+$ ) and  $\sim 41\%$  (in the case of  $H^-$ ) of the expected 92 mm internal pipe diameter of the second part of the LEBT.

The resulting beams at the output present an acceptable matching for the RFQ input specification. A better accuracy in matching the  $T\beta_i$  parameters has been imposed, in order to minimize the particle loss at the entrance of the RFQ [1]. This resulted in  $T\alpha_{xf} = 0.894$ ,  $T\alpha_{yf} = 0.865$ ,  $T\beta_{xf} = 0.030$  m/rad,  $T\beta_{yf} = 0.030$  m/rad for the  $H^+$  beam, and  $T\alpha_{xf} = 0.740$ ,  $T\alpha_{yf} = 0.467$ ,  $T\beta_{xf} = 0.0453$  m/rad,  $T\beta_{yf} = 0.0366$  m/rad for the  $H^-$ . In both cases, it is dif-

ficult to achieve a normalized rms emittance below  $\sim 0.6$   $\pi$ -mm-mrad without compromising the matching accuracy of the beam.

## ACKNOWLEDGMENTS

Special thanks to: D. Uriot, A. Leonardo and A. Zugazaga for their help.

## CONCLUSIONS AND FUTURE WORK

The upgradeability of the ESS-Bilbao Low Energy Beam Transport into a Y-shaped structure has been presented in the presented work. The only piece of equipment that is not available from the the previous design is a bending magnet. The presented layout has been based on the maximizing the reutilization of most of the components, as well as, minimization of the emittance growth and the particle loss, while matching the RFQ input requirements. Future work will study refined layouts such as, using shorter drift spaces to reduce the emittance growth.

## REFERENCES

- [1] I. Bustinduy, et al. "First LEBT Simulations For The Bilbao Accelerator Ion Source Test Stand", Proceedings of HB2010, Morschach, Switzerland, TH01B05, (2010).
- [2] "The New LEBT For The Spallation Neutron Source Power Upgrade Project" Proceedings of PAC07, Albuquerque, New Mexico, USA, TUPAS075 (2007).
- [3] Focusing of charged particles, Edited by Albert Septier (1967), Chapter 4.2.
- [4] COMSOL Multiphysics webpage, [www.comsol.com](http://www.comsol.com).
- [5] S. Jolly, et al. "Beam Diagnostics for the Front End Test Stand at Ral", DIPAC 2007, WEO02A01 (2007).
- [6] R. Duperrier, N. Pichoff, D. Uriot, "CEA Saclay codes review", ICCS conference, Amsterdam, (2002).